

Cite this: *Chem. Sci.*, 2024, **15**, 13937

All publication charges for this article have been paid for by the Royal Society of Chemistry

Received 6th July 2023
Accepted 17th July 2024

DOI: 10.1039/d3sc03466f

rsc.li/chemical-science

Introduction

Magnetic contrast agents, capable of enhancing image sensitivity within a MRI scan, are central to the effective diagnosis (and consequent prognosis) of a very broad range of clinical conditions and disease states.¹ Nanoparticulate contrast agents (NP CAs) offer enhanced signal-to-noise ratios and high associated relaxivity over their molecular counterparts, enriching MR image acquisition, often with accompanying improved circulation times and lower doses (and thus potential for reduced toxicity).² Examples are rich in number and chemical flavour, being based on (super)paramagnetically doped scaffolds that are largely organic, exclusively inorganic, or hybrid in nature.^{3–5} In heralding a new era of disease specific reporting, many of these are able to respond to a desired environmental stimulus (such as pH, ions, or biomolecules).⁶ Paramagnetic liposomes are a potentially potent subclass of these, possessing high biocompatibility, and an associated capacity for payload incorporation within the interior cavity.⁷

Liposomal CAs have been synthesised either through the immobilisation of paramagnetic probes on the membrane surface, or by encapsulation of magnetic probes such as Gd-chelates within the intra-vesicular volume of the phospholipid bilayer. These approaches have supported the incorporation of a high associated payload of 10^4 to 10^5 molecular chelates,⁸ such as gadoteric acid (Gd-DOTA), that can promote T_1 contrast generation *in vivo*.⁹ A number of thermosensitive DPPC liposomes capable of supporting thermally activated T_2 relaxivity have also

been reported.^{9,10} In addition to these, iron oxide nanoparticles (IONPs) have been integrated within the intra-vesicle space facilitating T_2 contrast.^{11–13} The influence of water exchange (limited and/or thermally activated) across the lipid bilayer is highlighted in this prior work; contrast is limited by membrane water permittivity and, thus, potentially responsive to any bilayer fragmentation or change in rigidity (thermally or chemically imposed, such as through the integration of cholesterol).^{14,15} Where DPPC

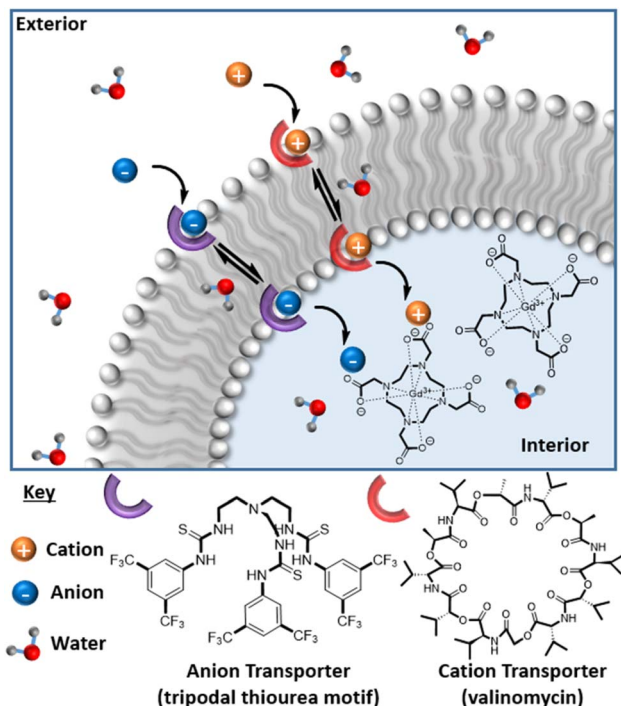


Fig. 1 A schematic illustrating the transfer of electrostatically bound K^+ to Vln and Cl^- by tripodal thiourea across the lipid bilayer of MR-active liposomes, accompanied by associated water transport which switches on MR image contrast.

^aDepartment of Chemistry, University of Oxford, South Parks Road, Oxford, OX1 3QZ, UK. E-mail: jason.davis@chem.ox.ac.uk; Fax: +44(0)1865272690; Tel: +44(0)1865275914

^bOxford Centre for Clinical Magnetic Resonance Research, Radcliffe Department of Medicine, University of Oxford, Level 0, John Radcliffe Hospital, Oxford, OX3 9DU, UK

† Electronic supplementary information (ESI) available. See DOI: <https://doi.org/10.1039/d3sc03466f>

‡ These authors contributed equally to this work.



liposomes have been loaded with both a therapeutic agent (Camptosar) and IONPs, thermally induced irreversible fragmentation enables both agent delivery and direct monitoring of this by T_2 weighted MRI.¹⁶

Ion channel mis-regulation is directly causative of several diseases; an ability to monitor exogenous ion imbalance *in vivo* would be beneficial for enhancing our understanding of these processes.¹⁷ Ion carriers capable of mediating transmembrane transport may offer valuable therapeutic intervention,^{18,19} and their development is an area of intense interest. Numerous synthetic ion transporters are known, including some that exhibit stimulus responsive behaviour.²⁰ Since ions are heavily solvated in aqueous solution,²¹ we hypothesised that recognition mediated transport would be accompanied by at least some associated exchange of water across the bilayer. We expected that this, in turn, would support a mechanistically novel platform for which image contrast switches in response to exogenous ions.

Results and discussion

MR active 1-palmitoyl-2-oleoyl-*sn*-glycero-3-phosphocholine (POPC) liposomes were here generated by a typical extrusion process, using a polycarbonate membrane with a pore size of 100 nm. POPC lipid membranes with incorporated cholesterol are highly biologically relevant, as they represent an idealised and highly tuneable model of the biomembrane.²² All liposomal samples exhibited high levels of colloidal stability ($PDI < 0.3$ for all samples), with an associated hydrodynamic size of 109.50 ± 4.51 nm and ζ -potential of -6.94 ± 0.71 mV for non-cholesterol modified POPC liposomes (POPC-C_{0%}-N) measured immediately after synthesis (as resolved by dynamic light scattering (DLS) measurements, ESI 9(a)†). Gd-DOTA was incorporated within the intra-vesicular cavity at the point of liposome formation, by dispersing the desired concentration of chelate in water and adding to the dried lipid film (ESI†). Resuspension, freeze-thawing and subsequent extrusion steps were conducted to afford the desired MR active vesicles (see the ESI† for procedure details). The liposomes were shown to be stable for 72 h, sufficient for MR analysis, with no significant differences in size or surface charge (ESI 9(a) and 9(b)†), observations of translational importance.²³ A range of Gd-DOTA loading densities were investigated (ESI 10†), with 75 mM ultimately added at the point of synthesis, to bias water exchange as rate limiting in relaxivity/contrast. These liposomes exhibited longitudinal relaxivity values ($r_1 = 4.70 \pm 0.02$ mM⁻¹ s⁻¹ at 1.41 T and 298 K, in water) characteristically indicative of effective diffusive water access across the lipid membrane. Notably, this water flux could be controllably “tuned down” significantly (at 1.41 T, associated $r_1 = 2.52 \pm 0.09$ mM⁻¹ s⁻¹, ESI 11†) by doping the bilayer membrane with 45 mol% cholesterol, (POPC-C_{45%}-N), a process associated with a negligible change in hydrodynamic size (99.35 ± 3.87 nm) and ζ -potential (-9.93 ± 1.12 mV) with a transmission electron microscopy (TEM) resolved diameter equal to 98.2 nm (ESI 12†). Good colloidal stability over 90 hours was also observed upon incubation of POPC-C_{45%}-N and POPC-C_{45%}-T in serum (ESI 13†) with no

significant variation in number mean. Osmotic shock experiments using DLS additionally confirmed the role of cholesterol in gating water flux (ESI 14†), whereby liposomes composed solely of POPC exhibited a ~20% reduction in the hydrodynamic diameter between incubation in pure water and 20 mM KCl solution. In comparison, liposomes doped with a high concentration of cholesterol (*i.e.*, >40%)²⁴ displayed no significant variation in size when subjected to the same conditions, confirming bilayer rigidification.

It is known that gramicidin-A (GramA) peptide channels can be reliably integrated into lipid bilayers, including those presented by liposomes, and are able to mediate water flux by a Grotthuss hopping mechanism at rates exceeding 10^{-6} cm⁻² s⁻¹ (Fig. 2(a)).^{25,26} The integration of GramA (2 mol% w.r.t. POPC) within the cholesterol modified liposomes was observed to support a very significant (>30%) boost in MR relaxivity for liposomes possessing 45–50 mol% cholesterol loading (Fig. 2(b)). Significantly, these experiments demonstrate that initially low liposomal contrast could be switched on if water flux across the bilayer is promoted.

We then sought to control (ion associated) water flux by integration of selective ion carriers within the liposomal

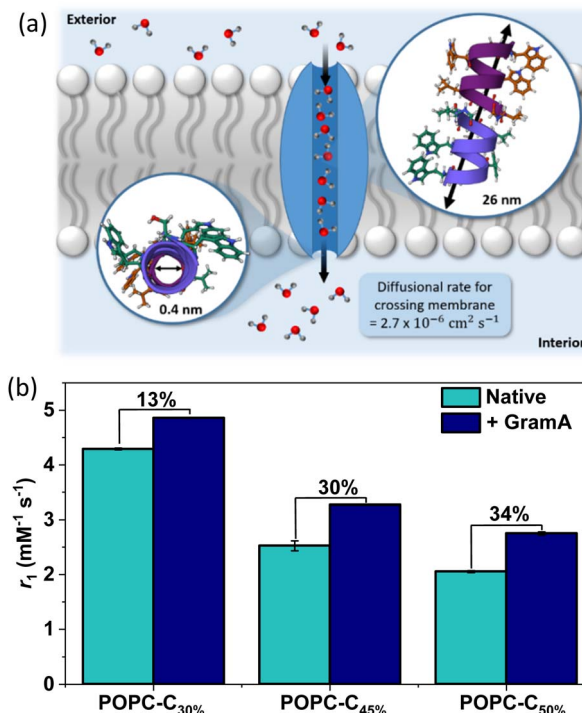


Fig. 2 (a) A schematic highlighting the transport of water molecules from the exterior solution to the interior pool of the liposomes, mediated by GramA (PDB ID: 1MAG).²⁶ The pore diameter and the length of GramA are 0.4 nm and 26 nm respectively, with the diffusion rate of water highlighted.^{25,26} The diameter of the pore channel is narrow and therefore it enables a single chain of 7–9 water molecules to align within it.²⁵ (b) The influence of GramA integration (2 mol% w.r.t. POPC) on the relaxivity (obtained at 1.41 T, 298 K) of pre-formed Gd loaded vesicles, across a range of cholesterol doping levels, to highlight the increased rigidification at higher cholesterol loading. Error bars for all data points were obtained from a linear regression analysis on linear plots of $1/T_1$ versus $[Gd^{(III)}]$ to obtain a value for the gradient, which is equal to $r_1 \pm 1$ s d.



membrane. Valinomycin (Vln) is an antibiotic of natural origin and an effective K^+ transmembrane transporter with rates in the region of 10^4 s^{-1} (Fig. 1).^{27–30} This K^+ ionophore, along with a tripodal thiourea anionophore developed by Busschaert *et al.* capable of efficiently transporting Cl^- ,³¹ were co-incorporated into the membrane of cholesterol-modified lipid vesicles (POPC–C_{45%}–T) by addition of a 1 mol% (w.r.t. POPC) DMSO stock solution to the liposome suspension. Extensive prior work supports non-destructive transporter integration by this method.¹⁹ Some water transport is known to be associated with the resultant ion transfer across the lipid bilayer.³² The rate of diffusion of water across an unmodified lipid membrane has been theoretically estimated to be 2×10^{-4} to $50 \times 10^{-4}\text{ cm s}^{-1}$ and is greatly reduced upon incorporation of cholesterol into the membrane (confirmed using stopped flow osmotic analyses).^{33,34} Given that the associated ion transport rates for the K^+ and Cl^- transporters used in this work are in the region of 10^2 to 10^4 s^{-1} , we anticipated a marked increase in water flux in their presence.^{27,31,32} Osmotic analyses herein confirm the coupling of anion/cation symport exchange across the bilayer to an enhanced water flux (see ESI 16†). Carrier mediated KCl symport (co-transport) and the associated increased water flux specifically correlate with an observable hydrodynamic size modulation as resolved by DLS (ESI 15 and 17†). Real time analyses of this (ESI 18†) enable an estimation of some 750% increase in net water flux when both mobile carriers are present (ESI 19†). Pleasingly, this carrier mediated transmembrane water flux leads to substantial (60%) relaxivity change; notably this is observed only in the dual integration of both transporters and in the presence of physiologically relevant levels of KCl *i.e.*, through the activation of net neutral K^+/Cl^- symport transport.³⁵ Integration of either the cation or anion transporter alone in the presence of the same levels of KCl results in no detectable change in relaxivity (ESI 20(a) and (b)†). The

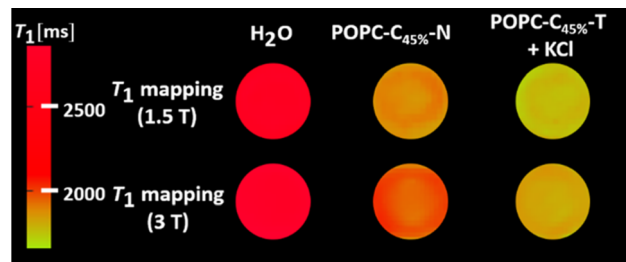


Fig. 4 T_1 weighted MRI maps, recorded at 1.5 T and 3 T (298 K) for the cholesterol doped lipids in the absence and presence of the transporters and KCl salt (1.08 mM).

requirement for KCl symport was also confirmed through ion transport experiments in liposomes using a fluorescence assay, which demonstrated that efficient Cl^- net flux in the presence of K^+ requires both the cationophore and the anionophore to be present (ESI 21†).³⁶

T_1 was independent of the KCl concentration across the physiological range (0.1–5.0 mM), consistent with the high activity of both ionophores (see ESI 22,† measured at 1.4 T).^{27,31,37} Assessing the anion selectivity of this we noted relative enhancements in r_1 of 83% and 67% were observed experimentally in the presence of 1.08 mM Br^- and NO_3^- respectively (see Fig. 3(b)), seemingly correlating with the ease of anion desolvation and hence transport efficiency.³¹ Cation selectivity trends were entirely consistent with the known Vln binding selectivities (see Fig. 3(a)).³⁸ Since molecular Gd chelates are used in approximately 40% of all MRI examinations,³⁹ we then demonstrated that this ion transport could generate significant image contrast change within T_1 weighted images obtained on a clinical MRI scanner (at 1.5 T and 3 T, at 298 K; Fig. 4). T_1 itself predictably increases for both POPC–C_{45%}–N and POPC–C_{45%}–T liposomes as magnetic field strength (B) increases (ESI 23†).

Building on the observations of ion flux mediated contrast switching with Gd-DOTA carrying liposomes, we integrated Gd-

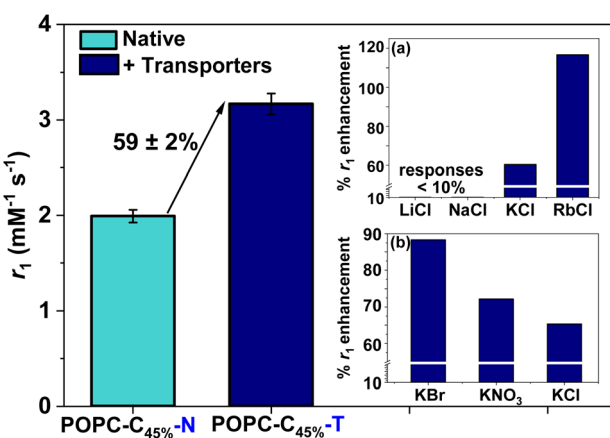


Fig. 3 Longitudinal relaxivity values obtained at 1.41 T, 298 K for 45 mol% cholesterol-doped liposomes in both the absence and presence of KCl (1.08 mM) and transporters (1 mol% each). Error bars represent 1 s.d. on either side of the mean r_1 value across two independent samples. Inset (a) shows the cation selectivity (1.08 mM MCl) with the greatest response observed for RbCl (~120%). Analogous Li and Na responses were <10%. Inset (b) displays the anion selectivity trend (1.08 mM KX).

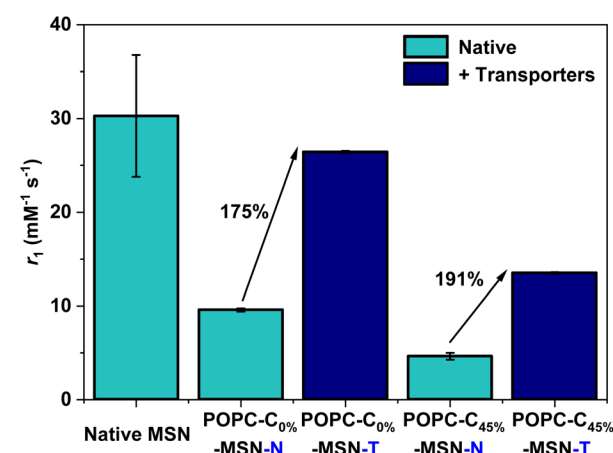


Fig. 5 r_1 values obtained at 1.41 T, 298 K for the POPC–MSNs (for 0 mol% and 45 mol% cholesterol modified bilayers), in both the absence and presence of the ionophores (1 mol% each), with the associated relative percentage switch in r_1 highlighted. Error bars are calculated as described in Fig. 2(b).

doped mesoporous silica nanoparticles (Gd-MSNs) into functional POPC liposomes (POPC-C₄₅–MSN–N) through fusion (ESI 7 and 8 for characterisation, and ESI 24–27†).⁴⁰ Characterisation by TEM and DLS confirms that these Gd-MSNs are consistently and effectively encapsulated within lipid bilayers, as expected.^{41,42} Since paramagnetic MSNs support much higher levels of relaxivity than molecular chelates,⁴ we hypothesised that the initial water transmembrane transport (and the small internal water pool) would be more limiting. Pleasingly, ion transport MR relaxivity turn-on is not only fully consistent with that observed with Gd-DOTA, but also indeed of a greater turn on magnitude; for both 0 and 45 mol% cholesterol doped lipid bilayers, relaxivity switches close to 200% were observed (Fig. 5) with Gd-MSN doped liposomes containing 1 mol% of both cation and anion transporters (POPC-C₄₅–MSN–T) in the presence of a 1.08 mM KCl gradient.

Conclusions

This work, then, demonstrates that the general principal of ion mediated water flux across the membrane of MR active liposomes is associated with significant modulation of MR relaxivity and associated image contrast. A “switch off” of paramagnetic liposome MR contrast can be established through lipid membrane rigidification and selectively re-established through water associated ion transport using synthetic ionophores. This proof of concept lays the groundwork for potentially imaging ion imbalance and the associated diseases thereof. Derivations which are both ratiometric (by, for example, integrating a cholesterol-anchored ¹⁹F probe)⁴³ and enzyme activated⁴⁴ can be envisaged.

Data availability

The data supporting this article have been included as part of the ESI.†

Author contributions

C. M. E., A. M. D., and H. L., designed the liposomes and acquired the experimental data. A. K. designed the liposomes and synthesised the tripodal thiourea anionophore. F. E. M. acquired the MRI data. M. J. L. and J. J. D. conceptualised and designed the project. C. M. E., A. M. D., M. J. L. and J. J. D. wrote the manuscript, which was approved by all authors.

Conflicts of interest

There are no conflicts to declare.

Acknowledgements

The authors would like to thank the following members of the Department of Chemistry, University of Oxford, for assistance: Lillian Leutloff for EM images, Dr Robert Barber for serum analyses, Xiangyu Chao with osmotic flux assays, James Smith with water flux assessments and Dr Manzoor Ahmad for

lucigenin ion transport studies. M. J. L. is a Royal Society University Research Fellow. A. M. D. would like to acknowledge funding from the EPSRC Centre for Doctoral Training in Inorganic Chemistry for Future Manufacturing (OxICFM), EP/S023828/1. A. K. acknowledges the EPSRC Centre for Doctoral Training in Synthesis for Biology and Medicine for a studentship (EP/L015838/1), generously supported by AstraZeneca, Diamond Light Source, Defence Science and Technology Laboratory, Evotec, GlaxoSmithKline, Janssen, Novartis, Pfizer, Syngenta, Takeda, UCB and Vertex.

References

- 1 J. Wahsner, E. M. Gale, A. Rodríguez-Rodríguez and P. Caravan, *Chem. Rev.*, 2019, **119**, 957–1057.
- 2 J. Pellico, C. M. Ellis and J. J. Davis, *Contrast Media Mol. Imaging*, 2019, **2019**, 1–13.
- 3 D. Ni, W. Bu, E. B. Ehlerding, W. Cai and J. Shi, *Chem. Soc. Rev.*, 2017, **46**, 7438–7468.
- 4 D. Yuan, C. M. Ellis and J. J. Davis, *Materials (Basel)*, 2020, **13**, 3795.
- 5 W. Zhang, L. Liu, H. Chen, K. Hu, I. Delahunty, S. Gao and J. Xie, *Theranostics*, 2018, **8**, 2521–2548.
- 6 C. M. Ellis, J. Pellico and J. J. Davis, *Materials*, 2019, **12**, 1–13.
- 7 Y. Xia, C. Xu, X. Zhang, P. Ning, Z. Wang, J. Tian and X. Chen, *Nanoscale*, 2019, **11**, 5822–5838.
- 8 A. L. Ayyagari, X. Zhang, K. B. Ghaghada, A. Annapragada, X. Hu and R. V. Bellamkonda, *Magn. Reson. Med.*, 2006, **55**, 1023–1029.
- 9 S. L. Fossheim, A. K. Fahlvik, J. Klaveness and R. N. Muller, *Magn. Reson. Imaging*, 1999, **17**, 83–89.
- 10 S. Y. Yeo, M. De Smet, S. Langereis, L. Vander Elst, R. N. Muller and H. Grüll, *Biochim. Biophys. Acta – Biomembr.*, 2014, **1838**, 2807–2816.
- 11 S. V. German, N. A. Navolokin, N. R. Kuznetsova, V. V. Zuev, O. A. Inozemtseva, A. A. Anis'kov, E. K. Volkova, A. B. Bucharskaya, G. N. Maslyakova, R. F. Fakhrullin, G. S. Terentyuk, E. L. Vodovozova and D. A. Gorin, *Colloids Surf.*, 2015, **135**, 109–115.
- 12 M. Meincke, T. Schlorf, E. Kossel, O. Jansen, C.-C. Glueer and R. Mentlein, *Front. Biosci.*, 2008, **13**, 4002–4008.
- 13 G. Béalle, R. Di Corato, J. Kolosnjaj-Tabi, V. Dupuis, O. Clément, F. Gazeau, C. Wilhelm and C. Ménager, *Langmuir*, 2012, **28**, 11834–11842.
- 14 M. K. Jain, D. G. Toussaint and E. H. Cordes, *J. Membr. Biol.*, 1973, **14**, 1–16.
- 15 R. Bittman and L. Blau, *Biochemistry*, 1972, **11**, 4831–4839.
- 16 Y. J. Lu, E. Y. Chuang, Y. H. Cheng, T. S. Anilkumar, H. A. Chen and J. P. Chen, *Chem. Eng. J.*, 2019, **373**, 720–733.
- 17 M. J. Langton, C. J. Serpell and P. D. Beer, *Angew. Chem., Int. Ed.*, 2016, **55**, 1974–1987.
- 18 P. A. Gale, J. T. Davis and R. Quesada, *Chem. Soc. Rev.*, 2017, **46**, 2497–2519.
- 19 L. E. Bickerton, T. G. Johnson, A. Kerckhoffs and M. J. Langton, *Chem. Sci.*, 2021, **12**, 11252–11274.
- 20 M. J. Langton, *Nat. Rev. Chem.*, 2021, **5**, 46–61.
- 21 E. J. Bieske, *Chem. Soc. Rev.*, 2003, **32**, 231–237.



22 V. V. S. Pillai, P. Kumari, A. Benedetto, D. Gobbo and P. Ballone, *J. Phys. Chem. B*, 2022, **126**, 4272–4288.

23 J. Schubert and M. Chanana, *Curr. Med. Chem.*, 2018, **25**, 4553–4586.

24 M.-L. Briuglia, C. Rotella, A. McFarlane and D. A. Lamprou, *Drug Deliv. Transl. Res.*, 2015, **5**, 231–242.

25 S. W. Chiu, S. Subramaniam and E. Jakobsson, *Biophys. J.*, 1999, **76**, 1939–1950.

26 R. R. Ketcham, K.-C. Lee, S. Huo and T. A. Cross, *J. Biol. NMR*, 1996, **8**, 1–14, PDB ID: 1MAG, DOI: [10.1007/BF01881753](https://doi.org/10.1007/BF01881753).

27 G. Stark, B. Ketterer, R. Benz and P. Läuger, *Biophys. J.*, 1971, **11**, 981–994.

28 S. K. Berezin, *J. Membr. Biol.*, 2015, **248**, 713–726.

29 A. Casnati, A. Pochini, R. Ungaro, C. Bocchi, F. Uguzzoli, R. J. M. Egberink, H. Struijk, R. Lugtenberg, F. De Jong and D. N. Reinhoudt, *J. Am. Chem. Soc.*, 1996, **2**, 436–445.

30 N. Gresh, C. Etchebest, O. de la Luz Rojas and A. Pullman, *Int. J. Quant. Chem.*, 1981, **20**, 109–116.

31 N. Busschaert, M. Wenzel, M. E. Light, P. Iglesias-Hernández, R. Pérez-Tomás and P. A. Gale, *J. Am. Chem. Soc.*, 2011, **133**, 14136–14148.

32 D. G. Levitt, S. R. Elias and J. M. Hautman, *Biochim. Biophys. Acta – Biomembr.*, 1978, **512**, 436–451.

33 T. H. Haines, *FEBS Lett.*, 1994, **346**, 115–122.

34 J. C. Mathai, S. Tristram-Nagle, J. F. Nagle and M. L. Zeidel, *J. Gen. Physiol.*, 2008, **131**, 69–76.

35 M. Zacchia, M. L. Abategiovanni, S. Stratigis and G. Capasso, *Kidney Dis.*, 2016, **2**, 72–79.

36 M. Chvojka, A. Singh, A. Cataldo, A. Torres-Huerta, M. Konopka, V. Šindelář and H. Valkenier, *Analysis Sensing*, 2024, **4**, e202300044.

37 S. Hoss, Y. Elizur, D. Luria, A. Keren, C. Lotan and I. Gotsman, *Am. J. Cardiol.*, 2016, **118**, 1868–1874.

38 Z. Su, D. Mrdenovic, S. Sek and J. Lipkowski, *J. Solid State Electrochem.*, 2020, **24**, 3125–3134.

39 J. Wahsner, E. M. Gale, A. Rodríguez-Rodríguez and P. Caravan, *Chem. Rev.*, 2019, **119**, 957–1057.

40 S. Mornet, O. Lambert, E. Duguet and A. Brisson, *Nano Lett.*, 2005, **5**, 281–285.

41 K. S. Butler, P. N. Durfee, C. Theron, C. E. Ashley, E. C. Carnes and C. Jeffrey Brinker, *Small*, 2016, **12**, 2173–2185.

42 P. N. Durfee, Y.-S. Lin, D. R. Dunphy, A. J. Muñiz, K. S. Butler, K. R. Humphrey, A. J. Lokke, J. O. Agola, S. S. Chou, I.-M. Chen, W. Wharton, J. L. Townson, C. L. Willman and C. Jeffrey Brinker, *ACS Nano*, 2016, **10**, 8325–8345.

43 J. Zhu, H. Zhang, K. Chen, Y. Li, Z. Yang, S. Chen, X. Zheng, X. Zhou and Z.-X. Jiang, *Adv. Healthcare Mater.*, 2020, **9**, 1901331.

44 M. Ahmad, T. G. Johnson, M. Flerin, F. Duarte and M. J. Langton, *Angew. Chem., Int. Ed.*, 2024, **63**, e202403314.

